MISSION-T2D

Multiscale Immune System SImulator for the Onset of Type 2 Diabetes integrating genetic, metabolic and nutritional data

Work Package 4

Deliverable 4.1

Report on Dynamic-E-MF model (minute-day time scale)

European Commission

SEVENTH FRAMEWORK PROGRAMME

Document Information

Grant Agreement	Nº	600803	Acronym	MISSION-T2D
Full Title	Multiscale Immune System SImulator for the Onset of Type 2 Diabetes integrating genetic, metabolic and nutritional data			
Project URL	http://www.mission-t2d.eu			
EU Project Officer	Name	Dr. Adina Ratoi		

Deliverable	No	4.1	Title	Report on Dynamic-E-MF model (minute-day time scale)
Work package	No	4	Title	Metabolic data provision and modeling of aggregated metabolic and inflammatory processes

Date of delivery	Contractual	01 Mar 2014	Actual	....
Status	Version 1.0.		Final	
Nature	Prototype		Report		Dissemination		Other	

Dissemination level	Consortium+EU	X
	Public	

Target Group (If Public)		Society (in general)	
Specialized research communities		Health care enterprises	
Health care professionals		Citizens and Public Authorities	

Responsible Author	Name	Albert de Graaf	Partner	TNO
	Email	albert.degraaf@tno.nl		

Version Log

Issue Date	Version	Author (Name)	Partner
27-2-2014	1.0	Albert de Graaf, Shaji Krishnan	TNO
28-2-2014	1.1	Albert de Graaf, Shaji Krishnan	TNO
28-2-2014	1.2	Filippo Castiglione	CNR

Executive Summary	This document describes the results of Tasks 4.1 and 4.2. Task 4.1 - The datasets available at partner TNO that are suited to calibrate the integrated metabolism-inflammation model at the minute-to-day timescale were identified. The datasets are described, and have been made available to the Consortium. Task 4.2 - The literature was searched for computational models of metabolism that can be interlinked with the agent-based inflammation model available at partner CNR. A best-suited model was selected and the corresponding software code was implemented. This model describes the influence of physical activity on metabolism. The structure of the model is described. Suggestions and mathematical equations for model extension to include model input from nutrient absorption are given. Tissue-specific basal inflammatory networks and major points of interaction between metabolism and inflammation were identified from literature search and are described. A prototypic mathematical model for insulin sensitivity modulation by adipose tissue inflammation was developed and the result of an example simulation is shown.
Keywords	data provision, computational model, dynamics of metabolism, physical activity, nutrient absorption, inflammation

Contents

1. Deliverable Description

Deliverable 4.1 is the result of Task 4.1: Data provision for models of the interaction metabolism, inflammation and physical activity, and Task 4.2: Modelling of the dynamics of the interactions between metabolism, inflammation and physical activity.

The objective of the two tasks is to develop an integrated dynamic energy-metaflammation (Dynamic-E-MF) model. This model should be at the mesoscopic inter-cellular scale, i.e., the tissue/plasma level, and describes the dynamics of tissue/organ aggregated metabolic and inflammatory processes and plasma markers roughly at the minute-day time scale.

Data to calibrate models at this level are typically taken from challenge tests. Suitable datasets were identified and made available as described in Section 2.1.

The focus of the work described in this report, i.e., the WP4 TNO contribution, is on building a dynamic model of human energy metabolism that should reflect the integrated regulation of metabolism in the fasted and postprandial state, as well as during physical activity, as discussed in [Frayn, 2009]. Several relevant models addressing this issue exist, but unfortunately all published models are limited in scope either because they address only a part of metabolism or because they focus only on a single organ. As an example, models focusing on the glucose-insulin dynamics [Dalla Man et al., 2007, Hill et al., 2013] and free fatty acid metabolism [Jelic et al., 2009] or combined [Roy and Parker, 2006, Xu et al., 2011; Pedersen et al., 2011] have been published but the dynamics of such important metabolites as TG, amino acids, ATP, ADP, NA(D)H, lactate and glycerol are not considered. Also, a detailed cellular kinetic model of liver metabolism [Koenig et al., 2012] was published which however is not linked to other organs. In fact only a single suitable model was identified that integrated both a more or less full set of metabolic pathways in cellular detail, and more or less complete whole body physiology. This model was published in [Kim et al., 2007] and is described in Sections 2.2.1 and 2.2.2. The model, since it is a physiologically based kinetic model, in principle is suited for integration with the agent-based inflammation model developed by partner CNR in WP6. In the meeting of February 2014 in Cambridge, the Consortium partners unanimously agreed that the model in [Kim et al., 2007] is the best model currently available to use as a starting point for developing the integrated metabolism-inflammation models.

Inflammation is a complex dynamic process with many factors involved. It is difficult to distinguish acute from chronic inflammation from any single observation since more or less the same set of inflammatory factors are involved. The interaction between inflammation and metabolism across various organs is an even more complex dynamic system with a great many potential influencing factors. We have investigated the literature to determine the most important organ-specific links between metabolism and inflammation, and to construct minimally complex networks that capture the essence of organ-specific inflammatory processes. These can be used as a basis to build a simulation model. A first generic demonstration model to simulate increasing insulin resistance with growing body mass was set up. The results of efforts done in Task 4.1 to model inflammation and its links with metabolism are described in Section 2.2.3.

The results Tables and Figures are assembled in Sections 3.1, 3.2 and 3.3.

2. Deliverable Results

2.1. Task 4.1. Data provision for models of the interaction metabolism, inflammation and physical activity

Data provision: TNO is currently involved in many systems biology projects. An inventory of datasets potentially useful for MISSION-T2D was made. The inventory includes basic study parameters and data type specification.

2.1.1. Datasets for the dynamic E-MF model

For the dynamic E-MF (i.e., energy metaflammation) model, the datasets shown in Table 1 were considered useful. The data was extracted and stored in a dedicated place on a TNO server for use by the Consortium.

2.2. Task 4.2. Modeling of the dynamics of the interactions between metabolism, inflammation and physical activity

Dynamics model: In the following, we describe in 2.2.1 the model of [Kim et al., 2007]. This model was principally developed to describe the dynamics of metabolic changes following physical exercise. In section 2.2.2 the extension of this model to include the metabolic dynamics associated with nutrient input following a meal is described. To date, an integrated model linking metabolism and inflammation does not exist. The first step to develop such a model is to identify the interaction points of metabolism and inflammation. These are discussed in section 2.2.3.

2.2.1. Description of the metabolic model of [Kim et al., 2007]

The basic physiological structure of the [Kim et al., 2007] model is shown in Figure 1. Metabolic functions and biochemical reactions differ from one tissue to another. The general tissue metabolic scheme is presented Figure 2, and metabolic functions specific to each tissue are shown schematically in Figure 3. A brief summarizing

description of the key concepts of the modelling approach is given below, together with selected example equations.

- **Metabolic flux equations:**

The basic model of Kim et al. [2007] use a generalized kinetic equation for any metabolic flux:

$$\phi_{x,X-Y\rightarrow V-W} = V_{x,X-Y\rightarrow V-W}\left(\frac{\frac{C_X}{K_X}\cdot\frac{C_Y}{K_Y}}{1+\frac{C_X}{K_X}+\frac{C_Y}{K_Y}+\frac{C_X}{K_X}\cdot\frac{C_Y}{K_Y}}\right)\left(\frac{PS^{\pm}}{\mu^{\pm}+PS^{\pm}}\right)\left(\frac{RS^{\pm}}{v^{\pm}+RS^{\pm}}\right)$$

where $V_{x,X\text{-}Y \rightarrow V\text{-}W}$, K_X and K_Y are Michaelis-Menten parameters specific to the reaction process, C_X and C_Y are concentrations of substrate X and Y in tissue x. In this expression, phosphorylation state, $PS^+ = C_{ATP}/C_{ADP}$, and redox state, $RS^\times = C_{NADH}/C_{NAD+}$. For some reactions, the effect of these controllers can be in the opposite direction. In this case, $PS_- = 1/PS_+$ and $RS^- = 1/RS^+$. In addition, $v^{\pm}$ and $\mu^{\pm}$ are parameters for metabolic controllers. The metabolic controllers include hormones such as epinephrine (of which the concentration rises upon exercise) and insulin (of which the concentration rises upon ingestion of nutrients, specifically glucose).

The kinetic equations for the metabolic reactions, and dynamic mass balance equations in tissue, 'x', where x stands for tissues: brain, heart, muscle, GI, liver, and adipose can be found in Appendix 1 and Appendix 2, of [Kim et al., 2007] respectively.

For example the kinetic equations for Liver for Glycolysis I (forward reaction), and Lactate oxidation (reverse reaction) are as follows:

- **Glycolysis I (forward reaction) example:**

GLC + ATP → G6P + ADP, where GLC is Glucose, G6P is Glucose 6 Phosphate, ATP is Adenosine triphosphate, and ADP is Adenosine diphosphate. The flux equations are

$$\emptyset_{\mathrm{Liver,GLC}\rightarrow\mathrm{G6P}} = V_{\mathrm{Liver,GLC}\rightarrow\mathrm{G6P}}\left(\frac{PS^{+}_{\mathrm{Liver}}}{\mu^{+}_{\mathrm{Liver}}+PS^{+}_{\mathrm{Liver}}}\right)\left(\frac{\frac{C_{\mathrm{Liver},GLC}}{K_{\mathrm{Liver},GLC}}}{1+\frac{C_{\mathrm{Liver},GLC}}{K_{\mathrm{Liver},GLC}}}\right)$$

where, $\mathrm{V_{Liver,GLC\rightarrow G6P}}$ = 0.765 mmol min-1 (Table 5, [Kim et al. , 2007]) and $\mathrm{K_{Liver,GLC}}$ = 10.0 (Table 6, [Kim et al., 2007]) are Michaelis-Menten parameters, and $\mathrm{C_{Liver,GLC}}$ = 8.0 (Table 4, [Kim et al., 2007]) is the concentration of GLC in liver.

The phosphorylation state is denoted by $\mathrm{PS^{+}_{Liver}} = \frac{\mathrm{C_{ATP}}}{\mathrm{C_{ADP}}}$, where $\mathrm{C_{ATP}}$ = 2.74, and $\mathrm{C_{ADP}}$ = 1.22 (Table 4, [Kim et al. , 2007]), while μ^{+}_{Liver} is the parameter for the metabolic controllers (to be discussed later in the document).

- **Lactate oxidation (reverse reaction) example:**

LAC + NAD^{+} → PYR + NADH, where LAC is Lactate, PYR is Pyruvate, NAD is Nicotinamide adenine dinucleotide, and NADH is reduced form of NAD. The flux equations are

$$\emptyset_{\mathrm{Liver,LAC}\rightarrow\mathrm{PYR}} = V_{\mathrm{Liver,LAC}\rightarrow\mathrm{PYR}}\left(\frac{RS^{-}_{\mathrm{Liver}}}{\gamma^{-}_{\mathrm{Liver}}+RS^{-}_{\mathrm{Liver}}}\right)\left(\frac{\frac{C_{\mathrm{Liver},LAC}}{K_{\mathrm{Liver},LAC}}}{1+\frac{C_{\mathrm{Liver},LAC}}{K_{\mathrm{Liver},LAC}}}\right)$$

where, $\mathrm{V_{Liver,LAC\rightarrow PYR}}$ = 1.92 mmol min-1 (Table 5, [Kim et al. , 2007]) and $\mathrm{K_{Liver,LAC}}$ = $\mathrm{C_{Liver,LAC}}$ = 0.82 (Table 6, [Kim et al. , 2007], Table 4, [Kim et al. , 2007], the metabolic fluxes, the Michaelis-Menten parameters $\mathrm{K_{Liver,LAC}}$ is set to the initial tissue concentration of the corresponding substrate unless reported in the literature). The redox state is denoted by $\mathrm{RS^{-}_{Liver}} = \frac{1}{\mathrm{RS^{+}_{Liver}}} = \frac{1}{\frac{\mathrm{C_{NADH}}}{\mathrm{C_{NAD}}}}$, where $\mathrm{C_{NADH}}$ = 0.05, and $\mathrm{C_{NAD}}$ = 0.45 (Table 4, [Kim et al. , 2007]), while $\gamma^{-}_{\mathrm{Liver}}$ is the parameter for the metabolic controllers (to be discussed later in the document).

- **Mass balance equations**

Given the flux equations, the dynamic mass balance for a substrate in tissue in tissue, 'x', where x stands for tissues: brain, heart, muscle, GI, liver, and adipose can

be described by Equation 1 in [Kim et al., 2007]. For the mass balance, a perfectly mixed lumped tissue-capillary compartment is assumed with blood/tissue distribution of metabolites that can cross the cell wall determined by blood/tissue partition coefficients. For example the dynamic mass balance for GLC in liver is:

$$V_{eff,Liver,GLC}\frac{dC_{Liver,GLC}}{dt} = \emptyset_{Liver,G6P\rightarrow GLC} - \emptyset_{Liver,GLC\rightarrow G6P}Q_{Liver}\left(C_{a,GLC} - \sigma_{Liver,GLC}C_{Liver,GLC}\right)$$

where $V_{eff,Liver,GLC}$ = $0.93V_{Liver} + \sigma_{Liver,GLC}\,(0.07V_{Liver})$ = 0.93*1.5 + 0.68*0.07*1.5 (Table 1←V_{Liver}, and Table 7←$\sigma_{Liver,GLC}$ of [Kim et al. , 2007]) is the effective volume of Glucose in the liver, $\emptyset_{Liver,G6P\rightarrow GLC}$ is the G6P to GLC metabolic reaction and $\emptyset_{Liver,GLC\rightarrow G6P}$ is the GLC to G6P metabolic reaction and $Q_{Liver}\left(C_{a,GLC} - \sigma_{Liver,GLC}C_{Liver,GLC}\right)$ is the net uptake and release rate of Glucose in Liver. Q_{Liver} is the blood flow to liver, $C_{a,GLC}$ = 5.0 (Arterial concentration of glucose for a normal overnight fasted human at rest, Table 2, [Kim et al. , 2007]), $\sigma_{Liver,GLC}$ = 0.68 partition coefficient of Glucose in liver (Table 7, [Kim et al. , 2007]) and $C_{Liver,GLC}$ concentration of Glucose in liver.

- **Glucagon-Insulin (metabolic hormone) controllers**

The maximum rate coefficient $V_{\mathrm{x,i}}$ in a metabolic reaction rate for liver is modulated by the glucagon-insulin ratio as given in Equation 6 of in [Kim et al., 2007]:

$$V_{x,i} = V_{x,i}^{0}\cdot\left(1.0 + \lambda_{x,i}^{G}\frac{(GIR(t) - GIR(0))^{2.0}}{\alpha_{x,i}^{G} + (GIR(t) - GIR(0))^{2.0}}\right)$$

where GIR is the ratio of arterial glucagon (C_G) and insulin ($_{CI}$) concentrations (GIR = C_G/C_I), and $\lambda_{x,i}^{G}$ and $\alpha_{x,i}^{G}$ are parameters for the GIR related effect. Since heart and skeletal muscles have no receptor for glucagon, they respond only to epinephrine. Thus the maximum rate coefficient for heart and skeletal muscles is modulated by epinephrine in a similar way as by the glucagon/insulin ratio as described in Equation 7 of in [Kim et al., 2007]. Similarly, the lipolysis in adipose and GI are modulated by epinephrine, and insulin levels. Hence the modulation of the maximum rate coefficients in metabolic reaction rates for adipose and GI is as described in Equation 8 of in [Kim et al., 2007].

- **Neural Activation of Metabolic Fluxes During Exercise**

To keep the arterial blood glucose concentration constant during exercise, the model implement a controller that affects circulating epinephrine levels, which then modulates glucagon and insulin secretion by the pancreas. The blood epinephrine level changes with a step increase in work rate according to an empirical relation show in Equation 9 of [Kim et al., 2007] whereas Equation 10 and Equations 11 describe the glucagon and insulin dynamics respectively.

- **Regional blood flow modulation by exercise**

In response to a step increase in work rate, blood flows in heart (H) and skeletal muscle (SM) increase, while blood flows in the gastrointestinal (GI) and liver (LI) tissues decrease. The blood flow for tissue x (= H, SM, GI, LI) changes according to:

$$Q_x(t) = Q_x(0) + \delta_x(1 - \exp(-t/\tau_Q))$$

where δ_x is a steady state gain for the blood flow change in tissue x, and τ_Q is a time constant. Blood flows to non-specified tissues are assumed to be constant during exercise.

- **ATP hydrolysis related to work rate**

The input to the whole body model during exercise is a step change of ATP hydrolysis rate ($\phi_{x,ATP\ ->\ ADP}$) in heart and skeletal muscle due to increased muscular work. For skeletal muscle, ATP hydrolysis rate depends on a work rate (WR) as

$$\phi_{m,\mathrm{ATP}\rightarrow\mathrm{ADP}}(\mathrm{WR}) = \phi_{m,\mathrm{ATP}\rightarrow\mathrm{ADP}}(\mathrm{rest}) + \gamma_m \cdot \mathrm{WR}$$

where gm is a conversion factor in skeletal muscle.

2.2.2. Nutrient input following a meal or challenge test.

The metabolic model of [Kim et al., 2007] was originally developed to describe metabolic changes that occur during exercise. It is here proposed to include nutrient input from meal ingestion in the dynamic model are described below.

- **Glucose absorption from a meal**

Dalla Man et al. [2007] describe the use of a physiological model of glucose intestinal absorption that had been recently developed [Dalla Man and Cobelli, 2006], and that is proposed to be integrated with the metabolic model of [Kim et al., 2007] described above.

Briefly, the intestinal absorption model describes the glucose transit through the stomach and intestine by assuming the stomach to be represented by two compartments (one for solid and one for triturated phase), while a single compartment is used to describe the gut as in the following equation taken from [Dalla Man and Cobelli, 2006]:

$$\begin{cases} Q_{\mathrm{sto}}(t) = Q_{\mathrm{sto1}}(t) + Q_{\mathrm{sto2}}(t) & Q_{\mathrm{sto}}(0) = 0 \\ \dot{Q}_{\mathrm{sto1}}(t) = -k_{gri} \cdot Q_{\mathrm{sto1}}(t) + D \cdot d(t) & Q_{\mathrm{sto1}}(0) = 0 \\ \dot{Q}_{\mathrm{sto2}}(t) = -k_{\mathrm{empt}}(Q_{\mathrm{sto}}) \cdot Q_{\mathrm{sto2}}(t) + k_{gri} \cdot Q_{\mathrm{sto1}}(t) & Q_{\mathrm{sto2}}(0) = 0 \\ \dot{Q}_{\mathrm{gut}} = -k_{\mathrm{abs}} \cdot Q_{\mathrm{gut}}(t) + k_{\mathrm{empt}}(Q_{\mathrm{sto}}) \cdot Q_{\mathrm{sto2}}(t) & Q_{\mathrm{gut}}(0) = 0 \\ Ra(t) = \frac{f \cdot k_{\mathrm{abs}} \cdot Q_{\mathrm{gut}}(t)}{\mathrm{BW}} & Ra(0) = 0 \end{cases}$$

In this system of equations, Q_{sto} (mg) is the amount of glucose in the stomach (solid, Q_{sto1} and liquid Q_{sto2} phase); Q_{gut} (mg) is the glucose mass in the intestine; k_{gri} (min^{-1}) is the rate of grinding; $k_{empt}(Q_{sto})$ (min^{-1}) is the rate constant of gastric emptying, which is a nonlinear function of Q_{sto} (see below) and k_{abs} (min^{-1}) is the rate constant of intestinal absorption; f is the fraction of intestinal absorption which actually appears in plasma; D (mg) is the amount of ingested

glucose; BW (kg) is the body weight; and R_a (mg/kg/min) is the appearance rate of glucose in plasma.

$k_{empt}(Q_{sto})$ is described by the formula:

$$k_{\text{empt}}(Q_{\text{sto}}) = k_{\min} + \frac{k_{\max} - k_{\min}}{2} \cdot \{\tanh[\alpha(Q_{\text{sto}} - b \cdot D)] - \tanh[\beta(Q_{\text{sto}} - c \cdot D)] + 2\}$$

Where parameters α and β are constrained by imposing that $k_{empt} = k_{max}$ for both $Q_{sto}=D$ and $Q_{sto}=0$:

$$\alpha = \frac{5}{2 \cdot D \cdot (1-b)} \quad , \quad \beta = \frac{5}{2 \cdot D \cdot c}$$

If c is small, the equation for $k_{empt}(Q_{sto})$ then simplifies to

$$k_{\text{empt}}(Q_{\text{sto}}) = k_{\min} + \frac{k_{\max} - k_{\min}}{2} \cdot \{\tanh[\alpha(Q_{\text{sto}} - b \cdot D)] + 1\}$$

More details can be found in [Dalla Man and Cobelli 2006].

The glucose absorption model has been identified on data as described in [Dalla Man et al. 2007]. Parameters k_{gri}, a and c , were fixed following [Dalla Man and Cobelli 2006], while the remaining parameters were estimated with sufficient precision. They are reported in Table 2 (Process: Rate of Appearance) for both the normal and type 2 diabetic subjects.
In the metabolic model, the glucose Ra can be introduced as an additional external input of metabolite glucose (GLC) to the arterial blood compartment.

- **Fat and protein meal absorption**

The rate of appearance of TG from fat ingestion and Ala (representing the total amino acid influx) from protein intake can be modeled using the same set of equations as for glucose but with different parameter settings. These will have to be determined from the data sets supplied in Task 4.1. If parameters cannot be determined with precision, simpler models of nutrient absorption (also described in [Dalla Man and Cobelli 2006]) i.e. using a smaller number of parameters, may be used.

2.2.3. Interactions between metabolism and inflammation.

Inflammatory processes are very dynamic (time, location and cell types) and very complex (one cytokine can have opposite functions depending on time, place and level of expression). Particularly the discrimination of chronic inflammation versus acute inflammation is very challenging, since the same set of mediators are involved in both phases of the inflammation. Whereas at the start, the concept was to identify a series of tissue-specific chronic inflammation marker sets for liver, muscle, adipose and pancreas, in acute and chronic conditions, in fact it became quickly clear that no such a thing would be possible to achieve.

The dynamic inflammatory response following a nutritional (oral glucose or fat load), exercise (acute work load) or inflammatory (intravenous LPS, TNF or IL-6 exposure) challenge test follows a generic time course consisting of an initial pro-inflammatory response, and a secondary anti-inflammatory response as shown in figure 4 [Calder et al., 2013].

Table 3 (also from [Calder et al. 2013]) indicates that after a nutritional challenge, transient increases in TNF, IL-6 and CRP as well as of soluble adhesion molecules (VCAM-1, ICAM-1, E-selectin, P-selectin) are observed.

It is extremely difficult to obtain from the literature a clear picture of the metabolic-inflammatory links on the acute timescale (minute to day). On the longer timescale, the concepts seem to be better evolved, e.g., as reviewed by [Calder et al., 2011] and [Lumeng and Saltiel, 2011]. The NLRP3 inflammasome is thought to play a pivotal role as discussed in [Wen et al., 2012].

The multisystem effects of diet-induced obesity (DIO) are linked to an imbalance in homeostatic and pro-inflammatory immune responses. Obesity triggers inflammatory pathways in the brain and adipose tissue that deregulate physiological responses that maintain insulin and leptin sensitivity. Over time, ectopic lipid accumulation in muscle, liver, and blood vessels activates tissue leukocytes, contributes to organ-specific disease, and exacerbates systemic insulin resistance. Cellular- and cytokine-mediated inflammation in pancreatic islets accelerates the progression toward diabetes.

The major metaflammation events per organ/cell type are tabulated in Tables 4 and 5.

Lumeng and Saltiel [2011] developed a useful schematic representation of the obesity-associated molecular pathways driving inflammation as given in Figure 5. Thus, the

major metabolic mediators of inflammation are omega-3 fatty acids, lipids, saturated fatty acids, and the hormone adiponectin.

Relevant literature indicates that metabolic inflammation associated with obesity mostly originates in the adipose tissue, in line with findings from TNO pre-clinical studies that identified a weight gain-associated rise of fat mass above a threshold limit in adipose tissue expandability as a key trigger of adipose tissue inflammation. The conceptual model of adipose tissue related inflammation is as shown in Figure 6. Increasing adiposity results in a shift in the inflammatory profile of adipose tissue macrophages (ATMs) as a whole from an M2 state to one in which classical M1 pro-inflammatory signals predominate. Prototypic mathematical equations were set up to model the dynamics of the balance of pro inflammatory (TNF-alpha-driven) vs. anti inflammatory (IL-13-driven) processes governing the M1/M2 macrophage ratio, which in turn drive the IL-6/IL-10 ratio responsible for decreasing insulin sensitivity upon expansion of adipose tissue as indicated by a rise of BMI above 25. This equation system can in principle simulate a decrease in adipose tissue insulin sensitivity following growing body mass as shown in Figure 7.

To guide the development of organ-specific metabolism-inflammation modelling, organ-specific inflammation networks were composed based on information in the literature. These networks are shown in Figure 8 a-f, along with the literature sources.

The information from the inflammatory networks, together with the information in Tables 3, 4 and 5 will be used by in the MISSION-T2D project to determine the most important metabolism-inflammation interaction points that are to be included in the modelling. The decision will also consider the optimal match with the content of the agent-based inflammation model developed by partner CNR in WP6. Then, generic mathematical equations for the selected interactions in the integrated model wiil be developed. In the dynamic E-MF model, the slowly evolving effect of obesity-induced inflammation on metabolism can probably be modelled as an amplitude modulation factor of the Michaelis-Menten Vmax parameter of the metabolic flux equation (see section 2.2.1) for the affected metabolic reaction.

3. Deliverable Results – Images, Tables & Graphics

This section contains the figures and Tables pertaining to deliverable 4.1.

3.1. Task 4.1 - Data provision -Table

Table 1 - Overview of data for the dynamic E-MF model

Nr	Study	Study group	Intervention	Challenge tests	Analytical platforms used
1	TNO-Foodmix	N=36 Male overweight	RCT 5 wk Anti-inflamm foodmix	High Fat Challenge	TNO metabolomics platform (GC-MS), main inflammatory cytokines, clinical chemistry, transcriptomics
2	ADMIT (TNO, and Dutch partners)	N=12 M/F healthy	LPS inflamm	OGTT, OLTT, OGFL (=sum)	Main inflammatory cytokines (MesoScale Discovery assays), oxylipids, clinical chemistry, transcriptomics of selected genes
3	EU-NutriTech	N=100 M/F overweight	20% Caloric restriction, optimal diet	OGTT, OLTT, Exercise	Lipidome, Clinical chemistry, Metabolite profiling, Multiplex proteome, Nutritional status, Inflammation status, Oxidative stress, Nuclear receptor activation
4	Humet	N=16 Healthy Males	none	OGTT	clinical chemistry, comprehensive metabolomics platform (Biocrates), proteins, transcriptomics

5	TNO-Diclofenac	N=16 Healthy Males	LPS inflammation + Diclofenac	OGTT	TNO metabolomics platform (GCMS), LCMS lipids, LCMS FFA, clinical chemistry, main inflammatory cytokines, transcriptomics, oxylipids

3.2. Task 4.2 - Metabolic and inflammation dynamics model - Figures

Figure 1 - Whole body system physiology diagram for metabolism.

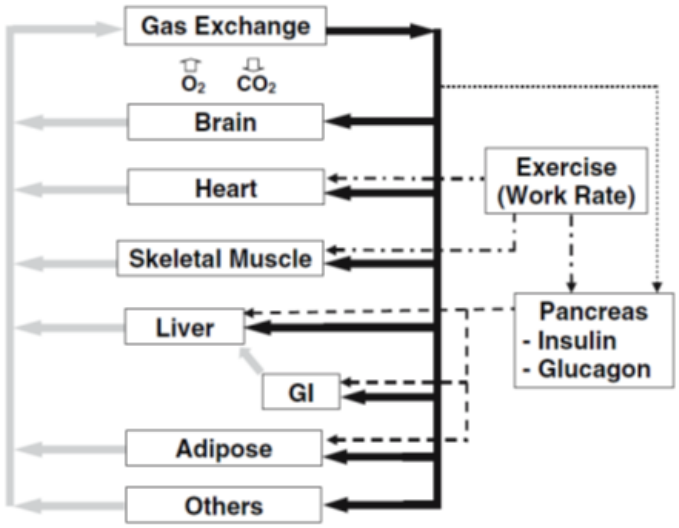

Each tissue is connected via the blood supply that carries substrates to organs/tissues in arterial blood (black solid arrows). Venous blood (gray solid arrows) leaving these tissues/organs takes away byproducts and becomes arterial blood to re-start the circulation after releasing carbon dioxide and taking up oxygen in lungs (gas exchange). Exercise sends neuroendocrine signals (dash-dot arrows) to heart, skeletal muscle and pancreas. In addition, feedback signal (dotted arrow) from the arterial glucose concentration can be sent to pancreas. Finally, glucagon–insulin ratio signal (dash arrow) from pancreas is sent to liver, GI (gastrointestinal) tract and adipose tissue. Taken from [Kim et al., 2007].

Figure 2 - General tissue metabolic pathways.

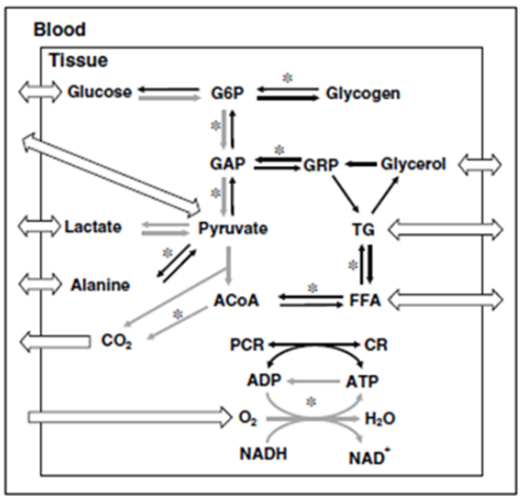

General metabolic pathways in whole body model. Nine substrates connected with open arrows are transported between tissue and blood. While gray arrows are common pathways in all tissues, black arrows are tissue specific pathways. The pathways marked with asterisk (*) are composed of several reaction steps but lumped into one step in this model. G6P: glucose-6-phosphate; GAP: glyceraldehyde- 3-phosphate; GRP: glycerol-3-

phosphate; TG: triglycerides; FFA: free fatty acid; ACoA: Acetyl CoA; PCR: phosphocreatine; CR: creatine. Taken from [Kim et al., 2007].

Figure 3 - Tissue-specificity of metabolic pathways.

Pathways	Brain	Heart	Muscle	GI	Liver	Adipose
Gluconeogenesis I, II, III (PYR→GAP,GAP→G6P,G6P→GLC)					■	
Glycogen synthesis (GLY→G6P)	■	■	■		■	
Glycogenolysis (G6P→GLY)	■	■	■		■	
Fatty acid synthesis (ACoA→FFA)					■	
Fatty acid oxidation (FFA→ACoA)		■	■		■	■
Lipolysis (TG→FFA+GLR)		■	■	■	■	■
TG synthesis (FFA+GRP→TG)		■	■	■	■	■
Glycerol Phosphorylation (GLR→GRP)		■	■		■	
GAP reduction (GAP→GRP)						■
GRP oxidation (GRP→GAP)					■	
Alanine breakdown (ALA→PYR)					■	
Alanine synthesis (PYR→ALA)			■			
PCR breakdown (PCR→CR)	■	■	■	■		
PCR synthesis (CR→PCR)	■	■	■	■		

Map for tissue specific metabolic pathways. In addition to the common pathways shown in Fig. 2, each tissue has different kinds of metabolic pathways. Blank filled with gray color means the existence of the corresponding pathway. GLC: glucose; PYR: pyruvate; GLY: glycogen; GLR: glycerol; ALA: alanine.

Figure 4 – Generic dynamic inflammatory response.

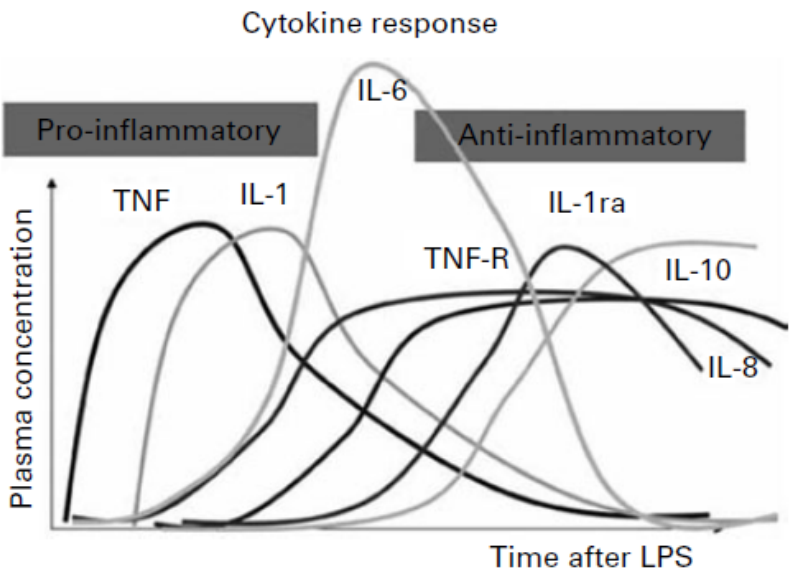

Generic time course of plasma cytokine concentrations after an inflammatory challenge (in this case a bolus intravenous injection of *Escherichia coli* lipopolysaccharide (LPS)). Concentrations and time are shown on arbitrary scales. There is an initial appearance of inflammatory cytokines (TNF and IL-1), followed by IL-6, and then anti-inflammatory cytokines (TNF receptor (TNFR), IL-1 receptor antagonist (IL-1ra) and IL-10). Taken from [Calder et al 2013]

Figure 5 – Molecular pathways in obesity-driven inflammation.

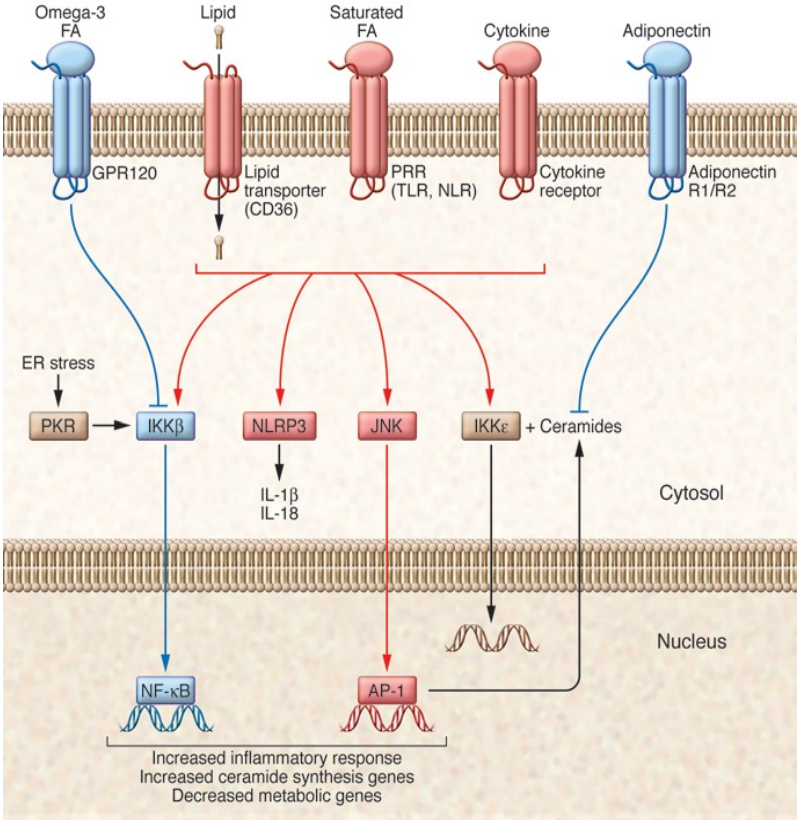

Molecular pathways at the interface between obesity and inflammation. Multiple signaling pathways participate in translating obesity-derived nutrient and inflammatory signals into a cellular response relevant in disease. These include proinflammatory (red) and antiinflammatory (blue) signals from the cell surface that integrate through many common intracellular pathways to generate the coordinated increase in inflammatory genes while repressing genes important in maintaining proper nutrient metabolism. PKR, RNA-dependent protein kinase. Taken from [Lumeng and Saltiel, 2011]

Figure 6 – Adipose tissue inflammation scheme.

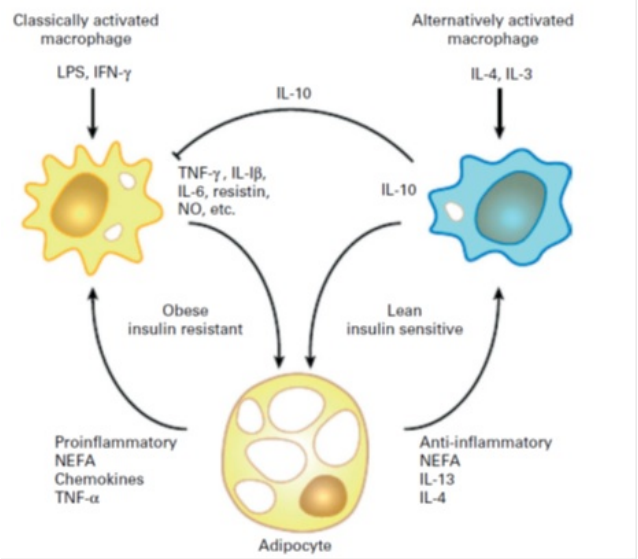

Schematic representation of factors regulating macrophage polarity and insulin resistance in adipose tissue. Under lean conditions, adipocytes secrete factors, such as IL-13, that promote alternative activation of macrophages. Alternatively activated (M2) macrophages secrete anti-inflammatory mediators, such as IL-10,

and may secrete insulin-sensitising factors. Obesity induces changes in adipocyte metabolism and gene expression, resulting in increased lipolysis and the release of pro-inflammatory NEFA and factors that recruit and activate macrophages, such as chemokines and TNF-a. Activated M1 macrophages produce large amounts of pro-inflammatory mediators, such as TNF-a, IL-1b and resistin, that act on adipocytes to induce an insulin-resistant state. This establishes a positive feedback loop that further amplifies inflammation and insulin resistance. IFN, interferon; LPS, lipopolysaccharide. Taken from [Calder et al., 2011].

Figure 7. Prototypic model of developing insulin resistance.

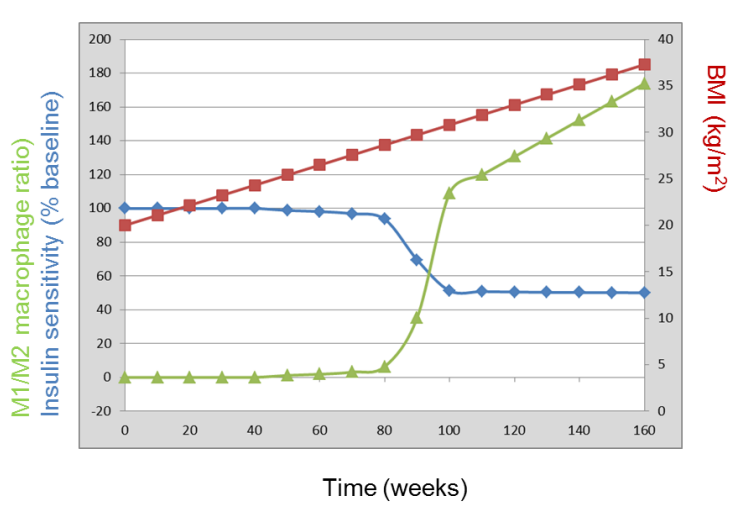

Simulation of decreasing insulin sensitivity resulting from a growing dysbalance of pro- and antiinflammatory processes in adipose tissue upon diet-induced obesity.

Figure 8a. Organ-specific inflammatory networks - Adipose tissue

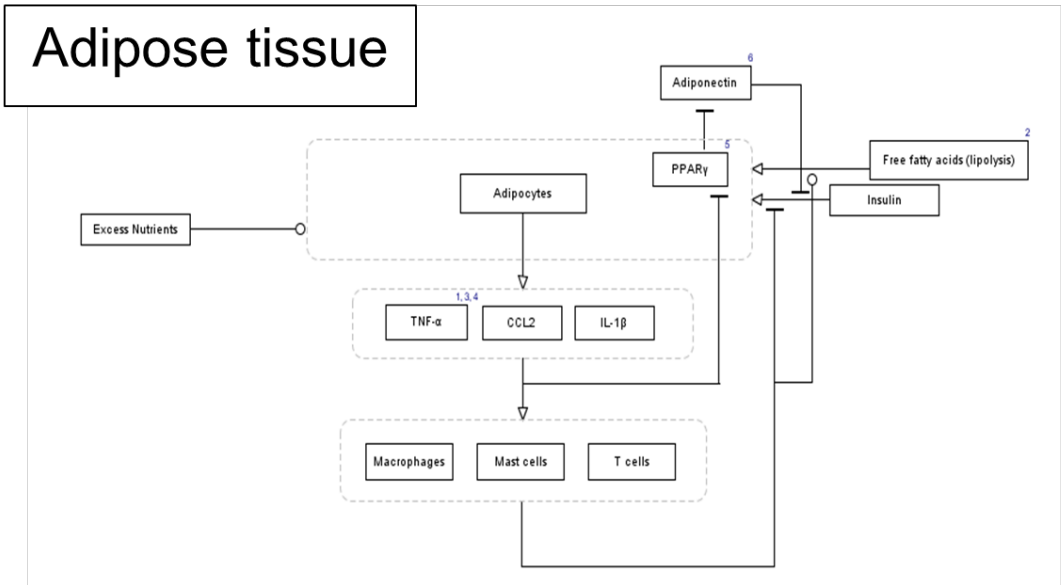

1. Tumor necrosis factor alpha-mediated insulin resistance, but not dedifferentiation, is abrogated by MEK1/2 inhibitors in 3T3-L1 adipocytes.; Engelman JA; Berg AH; Lewis RY; Lisanti MP; Scherer PE; Mol Endocrinol; 2000;
2. : Stimulation of lipolysis in cultured fat cells by tumor necrosis factor, interleukin-1, and the interferons is blocked by inhibition of prostaglandin synthesis.; Feingold KR; Doerrler W; Dinarello CA; Fiers W; Grunfeld C; Endocrinology; 1992;
3. Tumor necrosis factor alpha inhibits signaling from the insulin receptor.; Hotamisligil GS; Murray DL; Choy LN; Spiegelman BM; Proc Natl Acad Sci U S A; 1994;
4. Tumor necrosis factor-alpha-induced insulin resistance in 3T3-L1 adipocytes is accompanied by a loss of insulin receptor substrate-1 and GLUT4 expression without a loss of insulin receptor-mediated signal transduction.; Stephens JM; Lee J; Pilch PF; J Biol Chem; 1997;
5. Adipocyte dysfunctions linking obesity to insulin resistance and type 2 diabetes.; Guilherme A; Virbasius JV; Puri V; Czech MP; Nat Rev Mol Cell Biol; 2008;
6. : Adiponectin--journey from an adipocyte secretory protein to biomarker of the metabolic syndrome.; Trujillo ME; Scherer PE; J Intern Med; 2005;

Figure 8b. Organ-specific inflammatory networks – Liver

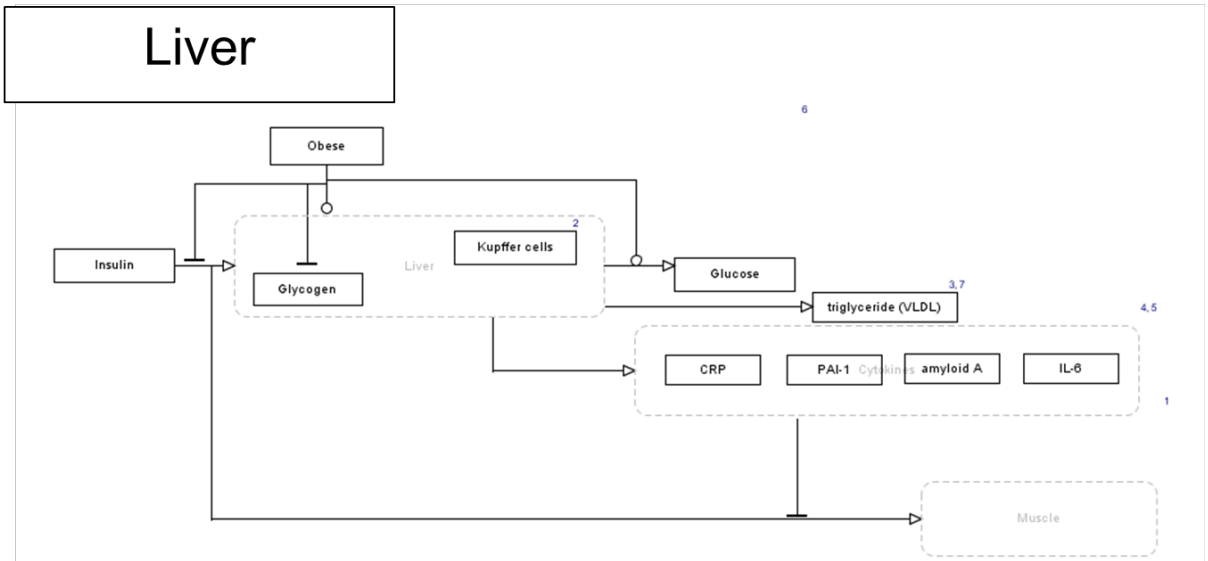

1. IKK-beta links inflammation to obesity-induced insulin resistance.; Arkan MC; Hevener AL; Greten FR; Maeda S; Li ZW; Long JM; Wynshaw-Boris A; Poli G; Olefsky J; Karin M; Nat Med; 2005;
2. Tumor necrosis factor-alpha suppresses insulin-induced tyrosine phosphorylation of insulin receptor and its substrates.; Feinstein R; Kanety H; Papa MZ; Lunenfeld B; Karasik A; J Biol Chem; 1993;
3. Inflammation and insulin resistance.; Shoelson SE; Lee J; Goldfine AB; J Clin Invest; 2006;
4. Is type II diabetes mellitus a disease of the innate immune system?; Pickup JC; Crook MA; Diabetologia; 1998;
5. Tumor necrosis factor-alpha stimulates hepatic lipogenesis in the rat in vivo.; Feingold KR; Grunfeld C; J Clin Invest; 1987;
6. Search for mediators of the lipogenic effects of tumor necrosis factor: potential role for interleukin 6.; Grunfeld C; Adi S; Soued M; Moser A; Fiers W; Feingold KR; Cancer Res; 1990;
7. Local and systemic insulin resistance resulting from hepatic activation of IKK-beta and NF-kappaB.; Cai D; Yuan M; Frantz DF; Melendez PA; Hansen L; Lee J; Shoelson SE; Nat Med; 2005;

Figure 8c. Organ-specific inflammatory networks – Pancreas

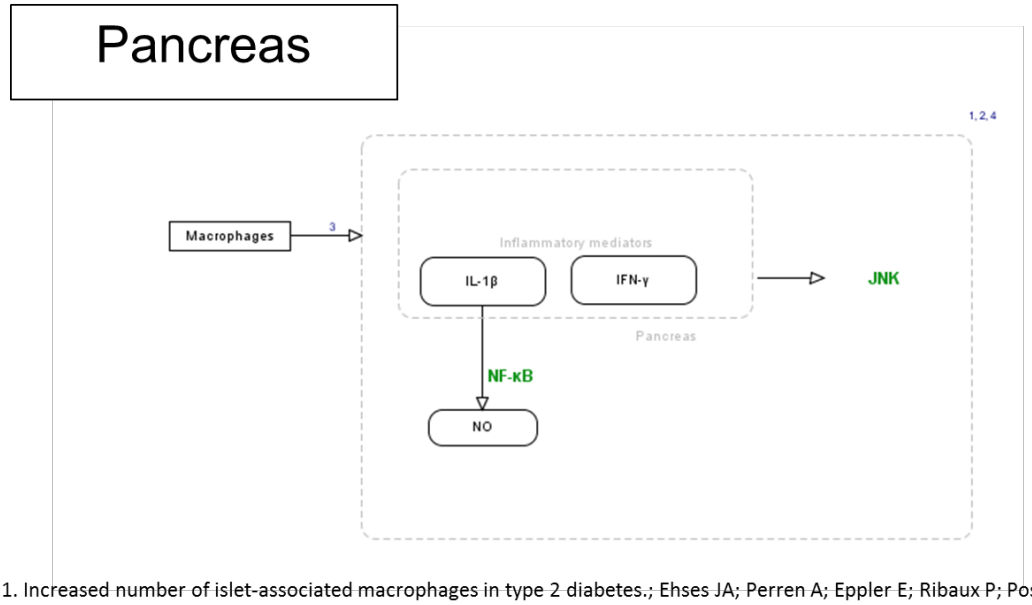

1. Increased number of islet-associated macrophages in type 2 diabetes.; Ehses JA; Perren A; Eppler E; Ribaux P; Pospisilik JA; Maor-Cahn R; Gueripel X; Ellingsgaard H; Schneider MK; Biollaz G; Fontana A; Reinecke M; Homo-Delarche F; Donath MY; Diabetes; 2007;
2. c-Jun amino terminal kinase 1 deficient mice are protected from streptozotocin-induced islet injury.; Fukuda K; Tesch GH; Nikolic-Paterson DJ; Biochem Biophys Res Commun; 2008;
3. Involvement of c-Jun N-terminal kinase in oxidative stress-mediated suppression of insulin gene expression.; Kaneto H; Xu G; Fujii N; Kim S; Bonner-Weir S; Weir GC; J Biol Chem; 2002;
4. Glucose and leptin induce apoptosis in human beta-cells and impair glucose-stimulated insulin secretion through activation of c-Jun N-terminal kinases.; Maedler K; Schulthess FT; Bielman C; Berney T; Bonny C; Prentki M; Donath MY; Roduit R; FASEB J; 2008;

Figure 8d. Organ-specific inflammatory networks – Brain

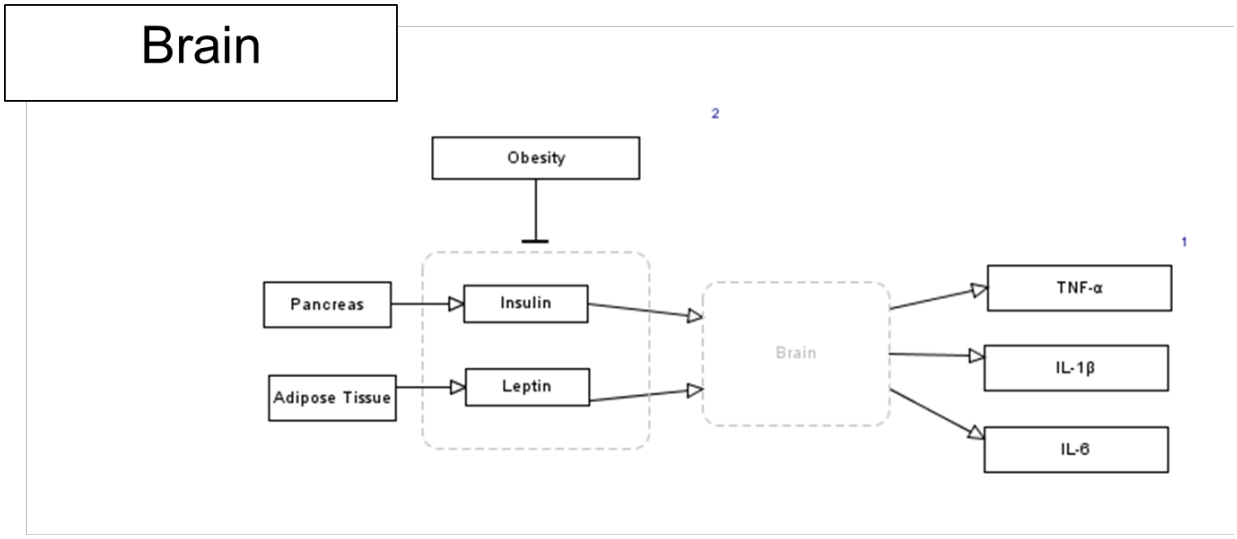

1. Minireview: nutrient sensing and the regulation of insulin action and energy balance.; Obici S; Rossetti L; Endocrinology; 2003;
2. Consumption of a fat-rich diet activates a proinflammatory response and induces insulin resistance in the hypothalamus.; De Souza CT; Araujo EP; Bordin S; Ashimine R; Zollner RL; Boschero AC; Saad MJ; Velloso LA; Endocrinology; 2005;

Figure 8e. Organ-specific inflammatory networks – Muscle

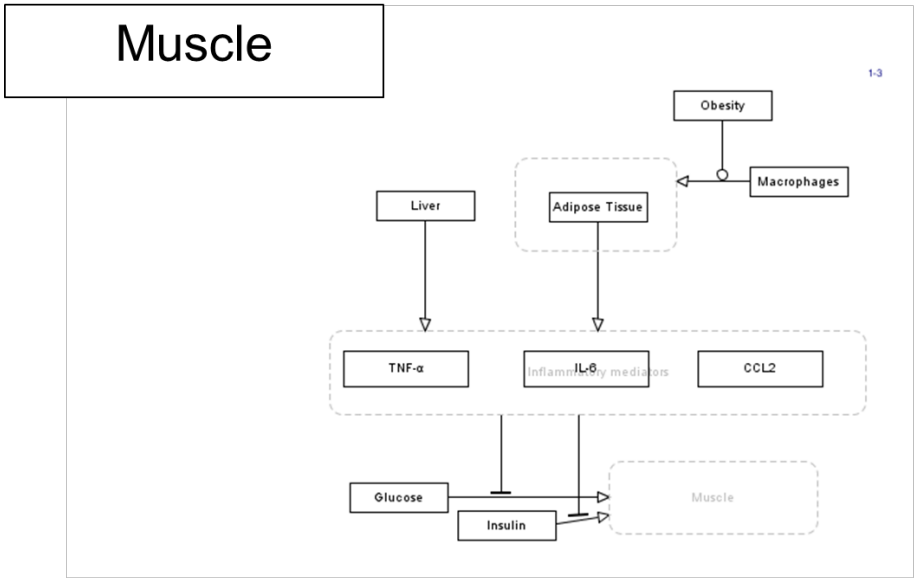

1. Serum retinol binding protein 4 contributes to insulin resistance in obesity and type 2 diabetes.; Yang Q; Graham TE; Mody N; Preitner F; Peroni OD; Zabolotny JM; Kotani K; Quadro L; Kahn BB; Nature; 2005;
2. Local and systemic insulin resistance resulting from hepatic activation of IKK-beta and NF-kappaB.; Cai D; Yuan M; Frantz DF; Melendez PA; Hansen L; Lee J; Shoelson SE; Nat Med; 2005;
3. Monocyte chemotactic protein-1 is a potential player in the negative cross-talk between adipose tissue and skeletal muscle.; Sell H; Dietze-Schroeder D; Kaiser U; Eckel J; Endocrinology; 2006;

Figure 8f. Organ-specific inflammatory networks – Intestine

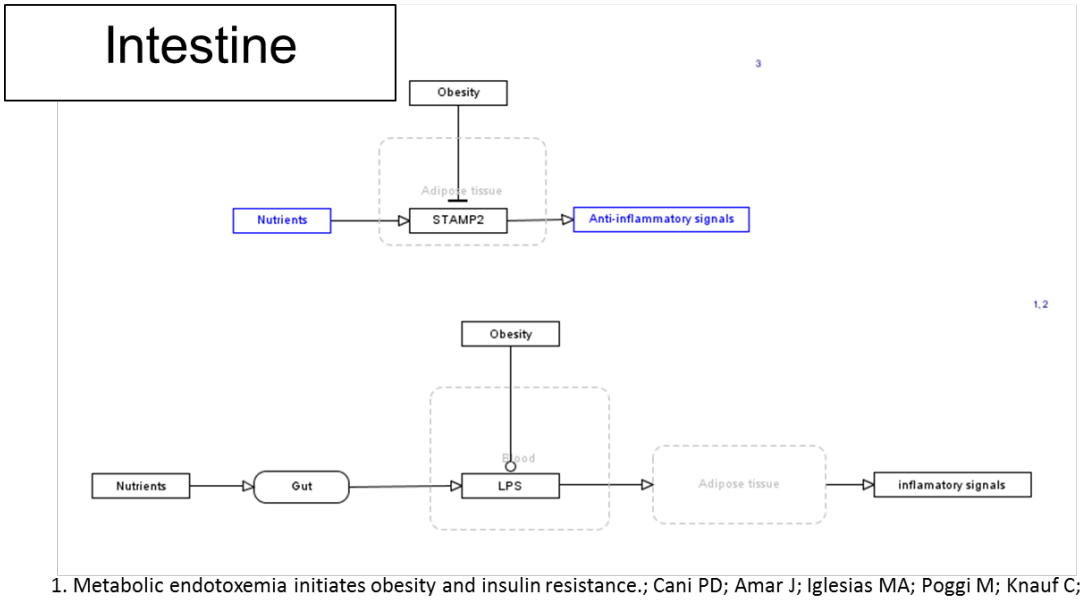

1. Metabolic endotoxemia initiates obesity and insulin resistance.; Cani PD; Amar J; Iglesias MA; Poggi M; Knauf C; Bastelica D; Neyrinck AM; Fava F; Tuohy KM; Chabo C; Waget A; Delmée E; Cousin B; Sulpice T; Chamontin B; Ferrières J; Tanti JF; Gibson GR; Casteilla L; Delzenne NM; Alessi MC; Burcelin R; Diabetes; 2007;
2. Coordinated regulation of nutrient and inflammatory responses by STAMP2 is essential for metabolic homeostasis.; Wellen KE; Fucho R; Gregor MF; Furuhashi M; Morgan C; Lindstad T; Vaillancourt E; Gorgun CZ; Saatcioglu F; Hotamisligil GS; Cell; 2007;
3. A high-fat meal induces low-grade endotoxemia: evidence of a novel mechanism of postprandial inflammation.; Erridge C; Attina T; Spickett CM; Webb DJ; Am J Clin Nutr; 2007;

3.3. Task 4.2- Metabolic and inflammation dynamics model - Tables

Table 2 Glucose absorption model parameters (taken from [Dalla Man et al., 2007])

Process	Parameter	Normal Value	Type 2 Diabetic Value	Unit
Rate of Appearance	k_{max}	0.0558	0.0465	min^{-1}
	k_{min}	0.0080	0.0076	min^{-1}
	k_{abs}	0.057	0.023	min^{-1}
	k_{gri}	0.0558	0.0465	min^{-1}
	f	0.90	0.90	dimensionless
	a	0.00013	0.00006	mg^{-1}
	b	0.82	0.68	dimensionless
	c	0.00236	0.00023	mg^{-1}
	d	0.010	0.09	dimensionless

Table 3. Challenge models that may be used to study an inflammatory response and their features. Taken from [Calder et al, 2013]

Challenge	Variability in design	Affected by	Effect on TNF*	Effect on IL-6*	Effect on CRP*	Effect on other mediators*
Oral glucose load	Modest (dose, time points, markers)	Obesity, T2D	↔ to ↑ (2–4 h)	↑ (2–4 h)	↑ (1 h)	↑ Soluble adhesion molecules
Oral fat load	High (amount and type of fat, time points, markers)	Obesity, T2D	↔ to -↑ (6 h)	↔ to ↑ (6–8 h)	↔ to ↑ (6 h)	↑ Soluble adhesion molecules, chemokines, cytokines (IL-8)
Acute exercise	High (duration and intensity of exercise, physical fitness, markers)	Age, physical fitness, presence of inflammatory disease	↔ to ↑	↔ to ↑	↔ to ↑	↑ Leucocytes, granulocytes
Intravenous administration of LPS, TNF or IL-6	High (type and dose of trigger, subjects, time points, markers)		↑ (2 h)	↑ (2–3 h)	↑ (24 h)	↑ Cortisol (4 h), noradrenaline (2 h), fever (4 h)
UVB exposure	High (type, dose and surface area of irradiation, time points, location)	UV dose (duration, wavelength), skin type	↔ (systemic) ↑ (6–12 h) (local)	↔ (systemic) ↑ (6–12 h) (local)		↑ IL-8 (6–12 h) ↑ IL-4, IL-10 (12–24 h), erythema, local eicosanoids
Vaccination	High (different vaccines, different study populations, time points)	Adjuvant used, CHD, depression, stress, T2D, age	↔ 3 h	↔ to ↑ (2 h to several weeks)	↑ (48 h)	↑ CCL2, eotaxin, IL-13, IL-2, IL-12, IL-15, total leucocytes, lymphocytes and monocytes (1 month)
Skin text (DTH, contact sensitisation)	High (antigens/allergens)	Sensitisation, age, exercise	No detectable systemic effects			Induration

CRP, C-reactive protein; T2D, type 2 diabetes; LPS, lipopolysaccharide; CCL, chemokine (C–C motif) ligand; DTH, delayed-type hypersensitivity; ↑, positive association; ↓, negative association; ↔, no clear association.
*Times indicated in parentheses are the approximate times of the maximal plasma concentration of the marker.

Table 4. Main tissue-specific inflammatory consequences of Diet-Induced Obesity (DIO) mentioned in [Lumeng and Saltiel 2011], [Wen et al 2012] and [Frisard et al., 2010].

Tissue	Main metabolic tissue reaction to DIO	Main inflammatory effects
Brain (hypothalamus)	elevated ceramide, diacylglycerol and saturated fatty acid concentrations	activation of neuronal JNK and NF-κB signaling pathways
Pancreatic islets	elevated glucose concentration	increased IL-1β production
Liver	lipid accumulation (fatty liver)	increased M1/Th1 cytokines and quantitative increases in immune cells
Muscle	none mentioned	
Adipose tissue	ER stress, adipose tissue hypoxia, and adipocyte death	coordinated inflammatory response
Intestine	microbial translocation?	modestly increased (0–200 pg/ml) circulating plasma endotoxin levels in states of obesity, type 2 diabetes, or in response to high fat feeding

Table 5. Main tissue-specific metabolic consequences of DIO-associated inflammation mentioned or referred to in [Lumeng and Saltiel, 2011].

Tissue	main tissue reaction to inflammation	main metabolic effects
Brain (hypothalamus)	impaired leptin and insulin signaling	increased food intake and nutrient storage, impaired insulin release from β cells, impaired eripheral insulin action, and potentiation of hypertension
Pancreatic islets	Macrophage accumulation, cytokine production	reduced insulin secretion and triggering of β cell apoptosis

Liver	macrophage infiltration	insulin resistance
Muscle	respond to inflammatory signals via pattern recognition receptors (PRRs) such as TLR4, also macrophage infiltration occurs but may not be DIO-specific since intrinsically linked to muscle injury and repair	activation of TLR4 with low (metabolic endotoxemia) and high (septic conditions) doses of LPS results in increased glucose utilization and reduced fatty acid oxidation occurring in concert with increased circulating triglycerides. Glucose is preferred substrate even in presence of elevated fatty acids, thus leading to increased intramyocellular lipid accumulation; however also insulin resistance is mentioned as consequence
Adipose tissue	excess of 20–30 million macrophages accumulating with each kilogram of excess fat; accumulation of CD8+ T cells, Th1-polarized CD4+ T cells, and loss of Tregs	impaired insulin signaling and impaired lipogenic/adipogenic capacity leading to visceral fat expansion

4. Deliverable Conclusions

4.1. Data provision - Task 4.1.

The datasets available at partner TNO that are suited to calibrate the integrated metabolism-inflammation model at the minute-to-day timescale, were identified. The datasets are described, and have been made available to the Consortium..

4.2. Modelling of the dynamics – Task 4. 2.

The literature was searched for computational models of metabolism that can be interlinked with the agent-based inflammation model available at partner CNR. A best suited model was selected and the corresponding software code was implemented. This model describes the influence of physical activity on metabolism. Suggestions and mathematical equations for model extension to include model input from nutrient

absorption are given. Using literature research, tissue-specific basal charts of inflammatory processes were constructed and the major points of interaction between metabolism and inflammation were identified and are reported. A prototypic model of insulin sensitivity modulation by adipose tissue inflammation was developed.

4.3. Next Steps of Dynamic modeling

The described model has to be interfaced with the model of inflammatory responses following discussions with WP2 and WP3, and then will be calibrated with data derived e.g. from various challenge tests (glucose, lipids, LPS). The developed integrated dynamic energy-metaflammation (Dynamic-E-MF) model thus will allow simulating mixed metabolic and inflammatory system responses to challenge tests. Simulations with this model will be used to derive indices (e.g., ratio's of response parameters) that reflect the dynamic capacity of the system to restore metabolic and inflammatory homeostasis after a nutritional, exercise, or inflammatory challenge. Integrative measures over time (e.g., AUC) of metabolites (glucose, FFA, TG, etc.), hormones (insulin, glucagon, etc.), and/or inflammatory cytokines (IL-6, TNF-a, IL-1b,etc) or inflammatory cell counts can be used to construct indices that characterize the average system flexibility towards disturbances. These indices can then feed e.g. as parameter settings, into the higher aggregation level model to be developed in Task 4.3.

5. References

Calder et al. (2011). Dietary factors and low-grade inflammation in relation to overweight and obesity. British Journal of Nutrition, Volume 106, Supplement, pp S1-S78.

Calder et al. (2013). A Consideration of Biomarkers to be used for Evaluation of Inflammation in Human Nutritional Studies. British Journal of Nutrition, Vol. 109 Supplement, pp S1-S34.

C. Dalla Man and C. Cobelli (2006). "A system model of oral glucose absorption: Validation on gold standard data," IEEE Transactions on Biomedical Engineering, vol. 53, pp. 2472–2478.

C. Dalla Man, R.A. Rizza, and C. Cobelli (2007). Meal Simulation Model of the Glucose-Insulin System. IEEE Transactions on Biomedical Engineering, Vol. 54, pp1740-1749

Frayn, K. (2009). Metabolic Regulation - A human perspective. Third Edition. John Wiley & Sons.

M. Frisard et al. (2010). Toll-like receptor 4 modulates skeletal muscle substrate metabolism. Am J Physiology Endocrinol Metab Vol. 298 pp. E988–E998.

N. R. Hill, J.C. Levy, and D. R. Matthews (2013) Expansion of the HomeostasisModel Assessment of β-Cell Function and Insulin Resistance to Enable Clinical Trial Outcome Modeling Through the Interactive Adjustment of Physiology and Treatment Effects - iHOMA2. Diabetes Care, Vol. 36 pp. 2324-2330

K. Jelic, C.E. Hallgreen, and M. Colding-Jorgensen (2009) A model of NEFA dynamics with focus on the postprandial satate. J. Biomedical Engineering, Vol. 37, pp 1897-1909.

Kim, J., G.M.Saidel, and M.E.Cabrera (2007). Multi-scale computational model of fuel homeostasis during exercise: effect of hormonal control. Ann. Biomed. Eng 35:69-90.

C. N. Lumeng and A.R. Saltiel (2011). Inflammatory links between obesity and metabolic disease, J Clin Invest. Vol 121 pp. 2111–2117

M. Koenig, S. Bulik, and H.-G.Holzhuetter (2012) Quantifying the Contribution of the Liver to Glucose Homeostasis: A Detailed Kinetic Model of Human Hepatic Glucose Metabolism PLoS Computational Biology 8(6): e1002577

M. G. Pedersen, C. Dalla Man, and C. Cobelli (2011) Multiscale Modeling of Insulin Secretion. IEEE Transactions on Biomedical Engineering, Vol. 58, pp.3020-3023.

A. Roy and R. Parker (2006), Dynamic modeling of free fatty acid, glucose, and insulin: an extended “minimal model”. Diabetes Technology and Therapeutics, Vol.8, pp 617-626.

H. Wen et al.(2012) A role for the NLRP3 inflammasome in metabolic diseases—did Warburg miss inflammation? Nature Immunology Reviews Vo. 13 pp. 352-357.

K. Xu, K.T. Morgan, A. Todd Gehris, T.C. Elston, and S.M. Gomez (2011) A Whole-Body Model for Glycogen Regulation Reveals a Critical Role for Substrate Cycling in Maintaining Blood Glucose Homeostasis. PLoS Comput Biol 7(12): e1002272